LRP 632/99 April 1999

Fast Bolometric Measurements on the TCV Tokamak

I. Furno, H. Weisen, J. Mlynar, R.A. Pitts,
X. Llobet, Ph. Marmillod, G. Pochon

submitted for publication in

REVIEW OF SCIENTIFIC
INSTRUMENTS

Fast Bolometric Measurements on the TCV Tokamak

I. Furno, H. Weisen, J. Mlynar, R.A. Pitts, X. Llobet, P. Marmillod, G. Pochon

Centre de Recherches en Physique des plasmas, Association EURATOM-Confédération Suisse,

Ecole Polytechnique Fédérale de Lausanne, CH-1015 LAUSANNE, Switzerland

The design and first results are presented from a bolometric diagnostic with high temporal resolution recently installed on the TCV tokamak. The system consists of two pinhole cameras viewing the plasma from above and below at the same toroidal location. Each camera is equipped with an AXUV-16ELO linear array of 16 p-n junction photodiodes, characterized by a flat spectral sensitivity from ultraviolet to X-ray energies, a high temporal response (< 0.5 μs) and insensitivity to low energy neutral particles emitted by the plasma. This high temporal resolution allows the study of transient phenomena such as fast MHD activity hitherto inaccessible to standard bolometry. In the case of purely electromagnetic radiation, good agreement has been found when comparing results from the new diagnostic with those from a standard metal foil bolometer system. This comparison has also revealed that the contribution of neutrals to the foil bolometer measurements can be extremely important under certain operating conditions, precluding the application of tomographic techniques for reconstruction of the radiation distribution.

1.0 Introduction

Precise measurements of the total radiated power are of upmost importance for the study of heat transport in magnetically confined plasmas. On TCV (Tokamak a Configuration Variable)[1], the total radiated power is presently measured using a 64-channel system based on miniaturized, low-noise, metal foil resistor bolometers originally designed at the Max Planck Institut für Plasmaphysik in Garching[2]. The diagnostic allows tomographic reconstructions of the poloidal emissivity distribution with a spatial resolution of ~4 cm and a temporal resolution of ~10 ms, limited by the integration time of the metallic resistor bolometers. This rather low time resolution is the most restrictive limitation of standard bolometric techniques.

In recent years, progress in Silicon deposition technology has allowed the fabrication of p-n junctions without the creation of a dead layer region at the Si-SiO_2 interface[3]. These photodiodes (also known as AXUV photodiodes) exhibit near theoretical quantum efficiency down to very low photon energy, for which the oxide absorption is negligible. Moreover, unlike metal foil bolometers, these diodes are insensitive to low energy (< 500 eV) neutral particles which are expelled from the tokamak plasma edge as a result of charge exchange and recombination processes and which can transport an important amount of power out of the plasma. Boivin et al.[4] recently reported high spatial resolution measurements of this neutral emission, using a combination of AXUV photodiode and metallic foil bolometer arrays. In this paper we will describe the application of these new photodiodes to measurements on TCV tokamak.

2.0 Diagnostic design

The diagnostic system consists of two pinhole cameras viewing the plasma from above and below at the same toroidal location. Each camera is equipped with a linear array of 16 photodiodes corresponding to a fan of viewing lines (Fig. 1) resulting in a spatial resolution of ~1.5 cm at the vessel midplane. A single chord in the upper camera coincides with one of the eight chords provided by the lower foil bolometer camera and vice versa. This allows some degree of comparison between the line integrated measurements from both systems. The photodiode and foil bolometer cameras are installed at the same toroidal position on the TCV vacuum vessel.

The detailed design features of the pinhole camera are shown in Fig. 2. The back of the camera head consists of a flange with a built-in 40-pin electrical feedthrough (supplied by Caburn-MDC) made up of two parallel rows of 20 Iron-Nickel alloy pins (0.5 mm diameter) embedded in glass cylinders (1.5 mm diameter) providing electrical insulation between the flange and the pins. The latter are directly plugged into a ceramic socket allowing the detector array, equipped with female connectors, to be directly mounted without any need for in-vacuum wiring. The camera housing comprises three concentric stainless steel cylinders, with water flow in the innermost gap providing active cooling of the detectors during vessel bakeout. A stainless steel plate at the front of the camera, located a few cm behind the protective graphite tiles lining the vacuum vessel, serves as a heat shield. Electrical insulation between the camera housing at the torus earth potential and the head flange is ensured by an intermediate ceramic ring. A stainless steel cylinder in the camera interior fixes the detector to the ceramic socket through an intermediate plate and provides support

for the pinhole aperture of dimensions 10×1.5 mm. Precise shaping of the aperture edges with minimum thickness of 20 μm is obtained by electro-erosion.

Each camera is equipped with an AXUV-16ELO linear array of 16 p-n junction photodiodes produced by International Radiation Detectors (IRD)[5] and designed for applications in the ultraviolet, extreme ultraviolet and soft X-ray spectral regions[6]. These photodiodes are of compact design and yield high sensitivity (0.24 W/A) with near theoretical quantum efficiency over a wide range of photon energy[7]. The absence of carrier recombination at the Si-SiO_2 interface together with an extremely thin (4-8 nm) hard Silicon protective entrance window, make these photodiodes sensitive to photon energies down to 1 eV and thus allow plasma edge phenomena to be observed. The only reduction in quantum efficiency (< 70% at 8 eV) at low energies is due to the SiO_2 entrance window and is mainly for 6-50 eV photons, for which absorption in the oxide layer is non-negligible. For photon energies higher than 6 keV, the efficiency is limited by the photodiode thickness chosen for the TCV diagnostic (35-40 μm). The photodiodes are operated in unbiased mode and have a rise-time shorter than 0.5 μs[6], making measurements with high temporal resolution possible. Each detector of the array has a dedicated preamplifier located on a printed circuit board mounted at the back of the camera head as close as possible to the electrical feedthrough in order to minimize electromagnetic pickup. The preamplifiers are current to voltage converters, based on the OP37 operational amplifier, with transimpedance gain of 1.2 MV/A and of a bandwidth of 100 kHz. Preamplifier outputs are collected by twisted pairs, with a signal and ground for each photodiode, grouped in a single, 14-m-long shielded cable containing 18 pairs (16 signals and +/-15 V power supply).

The signals are filtered by a 3 pole low-pass, Bessel filter with a cut-off frequency of 40 kHz, corresponding to the Nyquist frequency of the acquisition system. Analog-to-digital conversion and data acquisition are performed by a transient recorder based on a Vanguard 16 bit VME-based ADC also used to acquire the data from the 200 channel, soft X-ray tomographic system on TCV. The transient recorder, housed in a standard VME rack, comprises 288 simultaneous A/D converters, grouped in three identical banks of 96 channels, each feeding a separated VBS bus and a 64 Msample memory board. The three modules are controlled by a SUN processor linked to the TCV tokamak data acquisition system via Ethernet. Signals are digitized at the maximum sustainable acquisition rate of 80 kHz and stored on a local 2 GB disk drive. Complete data storage for each discharge is impracticable so that the acquired signals are sampled down to 10 kHz with the option for higher frequency storage (up to 80 kHz) in multiple reduced time windows. For all acquisition processes with an effective sampling rate < 80 kHz, anti-aliasing bandwidth reduction is performed on the local processor using a non-causal, non-recursive FIR filter with linear phase response and steep cut-off slopes.

3.0 FIRST EXPERIMENTAL RESULTS

As has been recently reported[4], one important feature of AXUV photodiodes is their insensitivity to low energy neutrals, unlike standard foil bolometers which cannot distinguish between power lost from the plasma by electromagnetic radiation or by neutral particle emission. One way to compare the performance of the two systems is to observe the response of both to a transient, purely electromagnetic radiative event. This may occur by deliberate injection of impurities or when minute pieces of debris from the surrounding walls fall into the plasma. Since impurities

clearly seen in the rapid increase of $\overline{n_e}$ together with the reduction in the D_α emission (a monitor of the flux of particles leaving the plasma edge). A period of "mossy" Edge Localized Modes (ELMs)[8] begins at t=0.505 s, producing a small modulation (2% of amplitude) in the radiated power measured by the AXUV photodiode viewing the divertor region (a portion of this period is shown in the expanded view at the bottom left of Fig. 4).

During the ELM-free phase, the central photodiode signal increases approximately as the square of $\overline{n_e}$ (indicating the dominance of recombination and Bremsstrahlung radiation from the core plasma), whilst the edge channel signal amplitude remains constant following an initial fast rise after the L-H transition. Qualitatively, these relative differences are the result of an abrupt steepening of the temperature profile and an increase in the electron temperature itself near the plasma edge following the transition. As a consequence, rapid modifications occur to both the spatial location and absolute concentration of the impurity species responsible for the emission. To understand this behaviour quantitatively requires modeling of the impurity transport, necessitating detailed measurements of density and temperature profiles in the localized region where strong gradients occur.

The increase in $\overline{n_e}$ is interrupted by several large ELMs, visible as spikes in the D_α emission which expel particles and heat from the plasma on a ms timescale[9] and which are also easily observed in the AXUV signals (expanded view at bottom right, Fig. 4). Spikes in the radiated power of similar amplitude are also seen in those channels (not shown in Fig. 4) of the upper camera viewing the outer divertor strike zone. Although the lack of chords crossing the X-point region

reside in the TCV plasma for only ~20 ms giving rise to a characteristic pulse of emission, their contribution is easily distinguishable. One such event is shown in Fig. 3 which illustrates the time evolution of the detected power (after background subtraction) measured along the same line-of-sight by an AXUV photodiode (full line) and by a standard bolometer (dashed line). The high temporal resolution of the photodiode allows detailed observation of the impurity penetration and subsequent expulsion from the plasma. Fast heat pulse propagation following internal disruptive instabilities (sawteeth) is also clearly visible as spikes in the measured emissivity. The much slower temporal resolution of the bolometer, even after deconvolution (rise time ~ 20 ms, 2 kHz acquisition frequency), smooths out the time trace and such detail is lost. Using the AXUV signal to estimate the incident power on the detector due to the transient event, the corresponding metal foil bolometer signal can be simulated if its temporal response characteristic is known[2]. The result of such a calculation is also shown in Fig. 3 (dot-dashed line), demonstrating the excellent agreement between the two diagnostics for this special case of purely electromagnetic radiation.

An illustration of the AXUV photodiode performance is presented in Fig. 4 showing measurements obtained from a TCV diverted plasma (Fig. 4, right) in which a transition from a low confinement (L-mode) to a high confinement (H-mode) regime occurs. This discharge also offers a good opportunity to compare the absolute values of measurements from both bolometric systems. On the left of Fig. 4 the D_α emission is shown together with the line integrated central density $\overline{n_e}$, an AXUV photodiode signal from the bottom camera (channel #1) looking through the plasma edge at the outer midplane and one from the top camera (channel #2) viewing along a chord passing through the core plasma and the divertor leg. The L-H transition, occurring at t=0.445 s, is

prevents tomographic inversion of the data, comparison of these divertor viewing channels with those of the lower camera viewing the same region of plasma indicates the presence of a highly radiating region around the divertor strike point during each ELM. This is confirmed by tomographic inversion of the standard bolometric signals during the ELMing period. The amplitude of the spikes on the photodiode signals indicates that significant quantities of heat and particles are expelled in the divertor region during large ELMs.

For the same discharge, the absolute chord brightness measured by pairs of standard bolometer detectors and AXUV photodiodes viewing the plasma along the same lines-of-sight are compared in Fig. 5. The time variation of three ratios of the detector signals are plotted (see caption in Fig. 5) demonstrating the differences in response of the two diagnostics. In L-mode the power detected by the metal foil bolometers is significantly higher than that measured by the photodiodes. This difference is more pronounced when using the standard bolometer signal viewing the plasma from below to take the ratio (signal pair 3/2 in Fig. 5). During H-mode, agreement between the standard bolometers and the AXUV photodiodes is considerably improved; the ratio of detectors 1 and 4 is close to unity and the ratio of detectors 3 and 2 is significantly decreased. For the latter signal pair, however, the outburst of the ELM activity leads to a large increase in the ratio. One likely interpretation of this behaviour is in terms of low energy neutral losses, to which only the standard bolometers are sensitive[4]. Recycling of neutrals is generally higher in L-mode compared with H-mode, as indicated by the D_α emission. The ELM instability temporarily destroys the edge transport barrier formed during the H-mode, leading to an increase in neutral recycling. The latter is more intense in the divertor region of the plasma where the particle exhaust is concentrated during ELM activity. As a result, the lower standard bolometer sees a higher neutral flux and the ratio 3/2

increases. In contrast, the hot plasma core prevents the upper metal foil bolometer from seeing the neutral particle production localized in the divertor volume.

Considerable support for this interpretation comes from tomographic inversion of data from the standard bolometer camera signals. Reconstructions which are consistent with raw data are not possible in the cases such as those in Fig. 5 in which neutral emission is strongly poloidally localized. Those channels associated with long path lengths through the plasma give lower values than expected. The signal behaves as if the plasma is optically thick, indicating that neutral particles contribute substantially to the measured signal level.

In addition to their increased time response, the AXUV photodiodes therefore also promise to be an invaluable tool in helping to separate the component of the total power losses due to neutral particles. In view of the encouraging results obtained during these preliminary experiments third pinhole camera of identical design will be installed on a lower lateral port and used to view the divertor region of discharges similar to that shown in Fig. 5.

4.0 Conclusions

A prototype bolometric system using photodiode arrays without dead-layers as detecting elements has been developed for TCV. Measurements made with the new diagnostic are in good agreement with those from standard metal foil bolometers in the case of purely electromagnetic radiation and in plasmas where neutral particle fluxes are low. The high temporal resolution allows detailed monitoring of fast MHD phenomena (sawteeth and ELMs) hitherto inaccessible to standard bolometric techniques. The new photodiode arrays have already proven invaluable in highlighting the

important contribution of neutral particles to the total power measured by the standard bolometer cameras on TCV.

5.0 Acknowledgments

The authors acknowledge the contributions of TCV team as well as helpful discussion with R. L. Boivin, R. Corde and B. Joye.

This work was partly supported by the Swiss National Foundation for Scientific Research.

6.0 References

[1]F. Hofmann et al, *Plasma Phys. Control. Fusion*, 36 (1994), B277

[2]K. F. Mast et al., *Review of Scientific Instruments,* Vol 62, N. 3 (1991), 744-750

[3]Raj Korde and Jon Geist, *Applied Optics*, Vol. 26 N.24 (1987), 5284-5289

[4]R. L. Boivin et al., *Review of Scientific Instruments*, Vol 70, N. 1 (1999), 260-264

[5]International Radiation Detectors, 2545 W,237th St., Unt I, Torrance CA 90505-5229

[6]International Radiation Detector (IRD), main catalogue

[7]E. M. Gullickson et al., *Journal of Electron Spectroscopy and Related Phenomena*, 80, 313 (1996)

[8]H. Weisen et al., *Plasma Phys. Control. Fusion*, 38 (1996), 1137-1148

[9]H. Weisen H. et al., *Plasma Phys. Control. Fusion*, 38 (1996), 1415-1419

Figures

FIG. 1. Location and viewing chord geometry of the prototype fast bolometric system installed on TCV.

FIG. 2. Cross-section of the TCV pinhole camera: 1, 40-pin electrical feedthrough; 2, AXUV detector array; 3, insulating ceramic ring; 4, poloidally limiting aperture; 5, front plate heat shield; 6, intermediate ceramic socket; 7, water cooled spacing between inner walls; 8, TCV vessel.

FIG. 3. Time evolution of the baseline subtracted chord brightness following a purely electromagnetic radiative event, caused by a piece of falling debris in TCV discharge #15452 at t=0.82 s. The full line is the AXUV photodiode signal. The standard bolometer trace (dashed line) agrees well with the simulated response (dot-dashed line).

FIG. 4. Evolution of an ohmic H-mode in TCV. Right: plasma configuration at t=0.6 s together with two lines of sight of the fast bolometric system, from the upper (#2) and lower (#1) cameras. Left: From top to bottom: D_α emission, line integrated central density, a signal (channel#1) from an AXUV photodiode looking through the plasma edge, a signal (channel#2) from an AXUV photodiode viewing the divertor region, expanded view of "mossy ELMs" (left) and of large ELMs (right).

FIG. 5. Time evolutions of the absolute chord brightness measured by metal foil bolometers and by AXUV photodiodes for the same discharge as in Fig. 4. Right: plasma configuration at t=0.6 s together with the detector line-of-sight (standard bolometers, 1 and 3, AXUV photodiodes, 2 and 4) used for the comparison. Left: various chord brightness ratios.

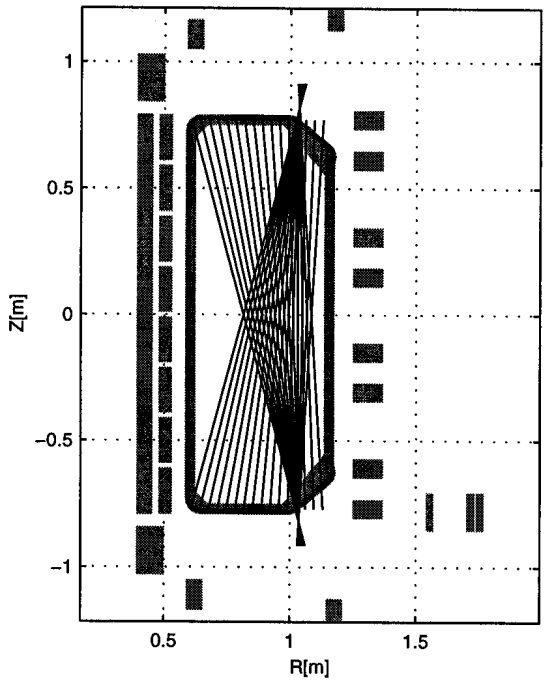

Figure 1

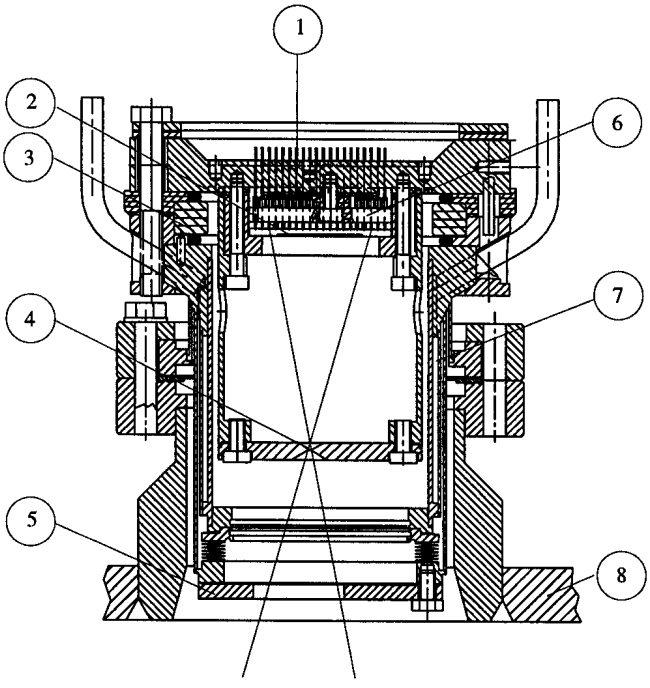

Figure 2

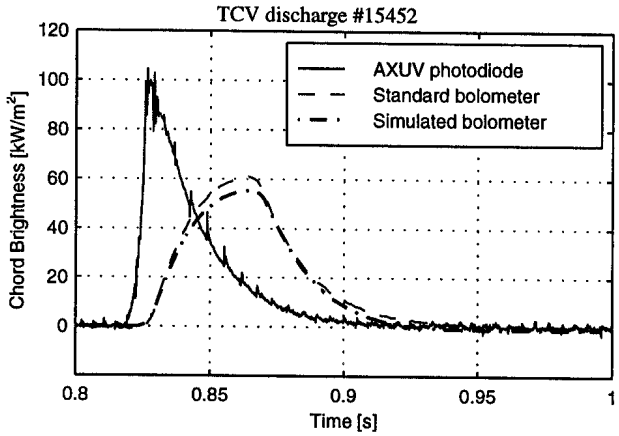

Figure 3

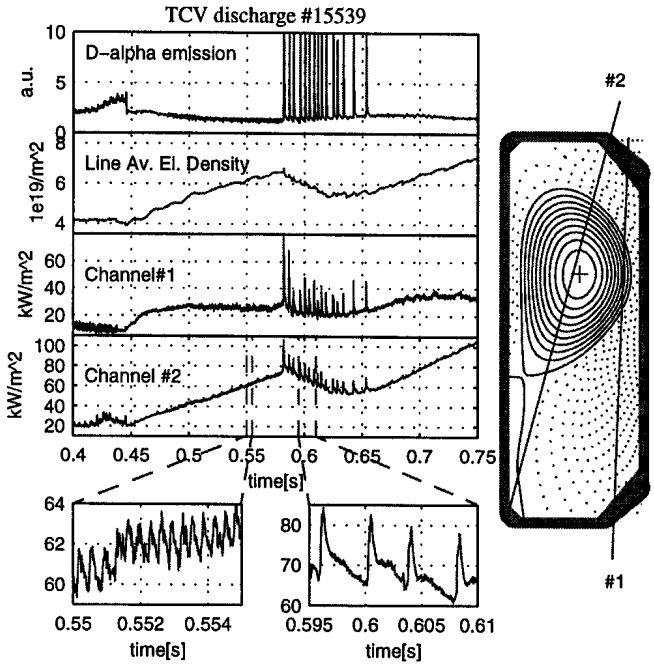

Figure 4

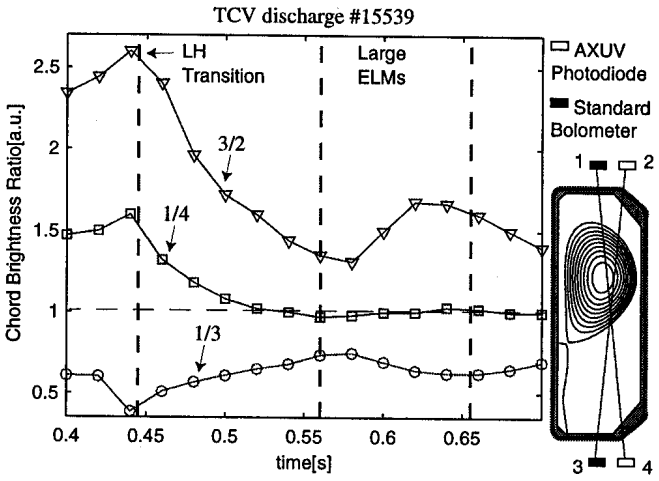
TCV discharge #15539
LH
Transition
Large
ELMs
AXUV
Photodiode
Standard
Bolometer
3/2
1/4
1/3
Chord Brightness Ratio[a.u.]
time[s]
2.5
2
1.5
1
0.5
0.4
0.45
0.5
0.55
0.6
0.65
1
2
3
4

Figure 5